Order-disorder transition at the (001) surface of a 3 at. %-Au-rich Cu_3Au crystal

S. B. Rivers* and W. N. Unertl
Department of Physics and Astronomy and Laboratory for Surface Science and Technology, University of Maine, Orono, Maine 04469

H. H. Hung† and K. S. Liang
Exxon Corporate Research Laboratory, Annandale, New Jersey 08801
(Received 12 June 1995; revised manuscript received 21 July 1995)

The order-disorder transition at the (001) surface of a 3 at. %-Au-rich Cu_3Au crystal has been studied using surface x-ray scattering and Auger-electron spectroscopy. Cu_3Au is a prototypical system for ordering alloys which undergo a first-order bulk phase transition. In contrast to previous studies on $Cu_3Au(001)$, we find that the order-to-disorder transformation at this Au-rich surface occurs at a temperature about 20 K *above* the bulk transition temperature ($T_{bulk}=644.5\pm2$ K). Changes in the near-surface composition during these transitions are less than 0.5%. Type-I antiphase domain boundaries, which leave nearest-neighbor configurations unchanged, form preferentially parallel to the surface. A phase is revealed with a large repeat distance normal to the surface and possibly involving type-II antiphase domain boundaries. The time dependence of the growth of the ordered domains during annealing times between 10^3 to 10^5 s was investigated through the x-ray measurement of the superstructure beam profile following a quench from the disordered state to a range of final temperatures in both the surface and bulk phases. In both cases the kinetics of the domain growth was substantially slower than the previously reported $t^{1/2}$ growth for the bulk. The nature of surface ordering is discussed in terms of surface segregation and formation of two types of antiphase domain boundaries.

I. INTRODUCTION

Alloys in the Cu-Au alloy system have been studied for decades as prototypes of systems that undergo an order-disorder transformation.[1] More recently, Cu_3Au surfaces have been studied as examples of systems with a continuous surface phase transition but a first-order bulk transition.[2–5] Lipowsky and co-workers have discussed the influence of the surface on order-disorder transitions for these systems in terms of wetting and drying transitions.[6,7] The time dependence, or kinetics, of the bulk Cu_3Au phase transition has also been studied extensively. However, the study of the kinetics of surface phase transitions on binary alloys has just begun in the last several years and the systems studied so far have been almost exclusively Cu_3Au surfaces. This is due in part to the extensive characterization of the Cu-Au alloy system in general and the Cu_3Au surfaces in particular.

In this paper we describe the order-disorder phase transition at the (001) surface of a Au-rich Cu_3Au single crystal. The specific composition is $Cu_{72}Au_{28}$. The composition of the surface region has been investigated as a function of temperature using Auger-electron spectroscopy (AES). The quasiequilibrium behavior and the effect of a surface on the first-order bulk phase transition of this sample have been investigated with grazing-incidence x-ray scattering (GIXS). The kinetics of the transformation were also studied with GIXS through a series of quenching experiments. These results are interpreted in terms of the interplay between the bulk and the surface and the formation of another phase in the coexistence region of the phase diagram. Preliminary reports of some of our results have been published.[8,9]

The paper is organized in the following order. In Sec. II, a brief review of previous publications relevant to our work is given. Section III describes the experimental methods employed in this study. The experimental results are presented in Sec. IV followed by discussions of the results in Sec. V. A summary is given in Sec. VI.

II. PREVIOUS STUDIES ON Cu_3Au

A. Cu-Au phase diagram

Figure 1 shows the portion of the Cu/Au phase diagram relevant to this paper. Cu and Au are completely miscible in the bulk in all concentrations above about 663 K. Below this temperature there are several ordered equilibrium structures depending upon the stoichiometry. Stoichiometric Cu_3Au has a first-order critical temperature T_{bulk} of about 663 K.[1] Below T_{bulk} the equilibrium phase is Cu_3Au I, an ordered cubic structure with Cu atoms occupying the face centers and Au atoms at the corner sites as shown in Fig. 2(a). The composition of adjacent {001} planes alternates between 50% Cu-50% Au and 100% Cu. The diffraction beams are observed for all Miller indices (hkl). Above T_{bulk}, the lattice sites are randomly occupied by Au and Cu atoms and all diffraction beams with mixed odd/even Miller indices become structure factor forbidden. Therefore, beams such as the (001) and (101) reflections provide a convenient way to monitor the bulk order-disorder transition. The beams that are forbidden above T_{bulk} are called *superstructure* beams, while those that are still observed are called *fundamental* beams.

Cu_3Au has two kinds of antiphase domains. Type-I antiphase domain boundaries involve half-diagonal glides in a $\langle 110\rangle$ direction. For example, in a 50% Cu-50% Au layer perpendicular to the a_1 direction, a slip of $(a_2+a_3)/2$ cre-

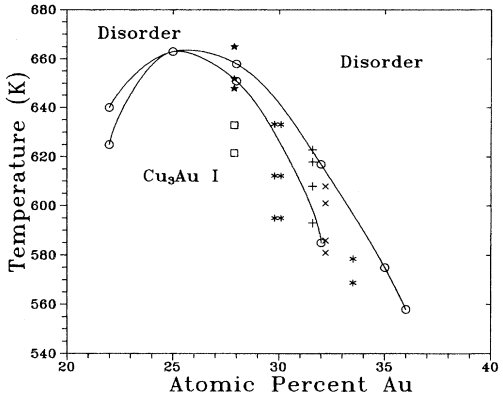

FIG. 1. The phase diagram of bulk Cu-Au near 25 at. % Au. Coexistence boundaries (○'s) are from Ref. 15. The other data points indicate regions with long-range periodic structures (stars and squares from this work, +'s from Ref. 16, ×'s, Ref. 17). See the text for details.

ates a type-I antiphase domain boundary. Since nearest-neighbor bonds are not changed by this type of antiphase domain boundary, the energy expense is small. Antiphase boundaries are most commonly studied by x-ray scattering since they cause characteristic changes in the shapes of the superstructure beams which, for the bulk, are analyzed in terms of two limiting cases.[10] One of these, illustrated in Fig. 2(b), assumes that the type-I antiphase domain boundaries are present in all symmetry equivalent orientations and form with equal probability at every lattice site. In this case, the broadening is anisotropic, forming diamond shaped "disks" of intensity at each superstructure position.[11,12] In the other limit, the type-I antiphase domain boundaries are assumed to have good long-range order, in which case the intensity of each sheet is replaced by four distinct beams centered at the location of each superstructure beam as illustrated in Fig. 2(b) by the crosses around the (010) reciprocal-lattice point. We show below that neither of these limiting cases describes the behavior we observed near the (001) surface.

The second kind of antiphase domain boundary is referred to as type II and occurs whenever two adjacent layers in a ⟨001⟩ direction have the same composition rather than alternating as for the perfect Cu_3Au I crystal structure. Due to their higher energy cost, they are expected to be less likely to form than type-I antiphase domain boundaries. But, once formed, they will be more difficult to remove. We present evidence below for a bulk phase in our sample involving type-II antiphase domain boundaries.

For concentrations that are Au- or Cu-rich with respect to Cu_3Au, there is a coexistence region between the solid solution and Cu_3Au I phases. A long-range periodic structure comprised of a periodic arrangement of type-I antiphase domain boundaries occurs in the coexistence region on the Au-rich side, but not on the Cu-rich side.[13] It is called Cu_3Au II, in analogy with the well-studied and theoretically explained long-range periodic structure of CuAu II.[14] Previous experimental data relevant to the phase diagram are summarized in Fig. 1. The points for the coexistence curves (circles) are taken from resistivity data,[15] the +'s from Scott,[16] and ×'s from Yakel[17] give the temperatures at which phase changes

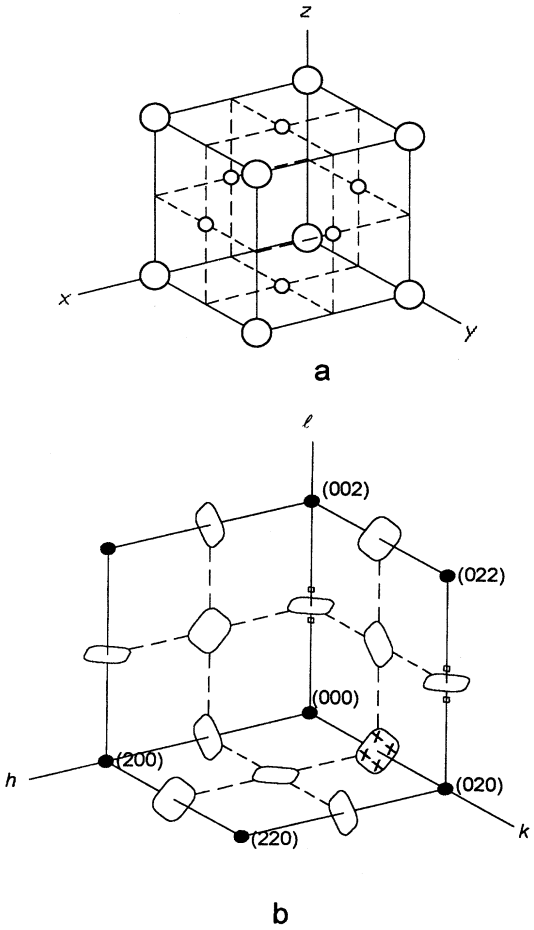

FIG. 2. (a) The low-temperature unit cell of bulk Cu_3Au I. (b) A portion of the reciprocal lattice of bulk Cu_3Au II. The solid dots are the fundamental beams observed at all temperatures. The diamond-shaped diffraction "disks" are centered on the positions of the superstructure beams and occur for the Cu_3Au II phase. Each disk sharpens into four points (×'s) if well-ordered arrays of type-I antiphase domain boundaries are present. Also shown (small squares) are the relative locations of the satellite reflections for a new phase (see text).

were observed by x-ray diffraction. In the direction of increasing temperature the points separate regions of Cu_3Au I, Cu_3Au I plus Cu_3Au II, Cu_3Au II, Cu_3Au II plus solid solution, and solid solution. Although the results are generally similar, discrepancies in the reported phase boundaries and transition temperatures exist. Several results from our quasi-equilibrium studies are also included (filled stars and squares) in Fig. 1 and will be discussed below.

B. Cu_3Au surfaces

Although previous studies of the surfaces of Cu_3Au indicate that the low index surfaces behave quite differently from the bulk,[2–4,8,18–30] many issues remain unresolved due to contradictions among the measurements. For example, on the question of the surface order-disorder transition, early examinations of the (001) surface using low-energy electron diffraction (LEED) and AES (Refs. 25 and 26) showed that the

surface ordered phase is the same as in the bulk, but that its phase transition was continuous rather than first order. Another LEED study on (001) (Ref. 2) was unable to distinguish whether the surface transition was continuous or partly discontinuous (with T_{surf} about equal to T_{bulk} in agreement with Sundaram *et al.*[25]). Subsequently, other investigations using spin-polarized LEED found the surface transition to be continuous.[3,4] Jamison *et al.*[3] also reported evidence for residual local order in the top layer above T_{bulk}. Alvarado *et al.*[4] interpreted their results in terms of a critical wetting transition. This interesting conclusion has also been described theoretically.[6,7] Later, x-ray evanescent-wave scattering by Dosch *et al.* from the sample used in Ref. 4 produced evidence for critical wetting by a surface-induced disordered layer below T_{bulk}.[5] We note that the composition of this sample is 1.5% rich in Cu.[20] Such small differences in sample composition may explain some of the discrepancies among published experimental results. For example, a grazing incidence x-ray scattering study by Liang *et al.* of a stoichiometric Cu_3Au sample[31] showed that an ordered surface layer persists at temperatures above T_{bulk}, in contrast to the surface disorder observed on the Cu-rich sample.[5]

The surface composition of an alloy may change as a function of temperature and this could also influence any phase transition. In the case of Cu_3Au (001) below the bulk transition temperature T_{bulk}, the surface is terminated by a layer with composition very near 0.5 Au and 0.5 Cu and the next layer is very close to 100% Cu as expected from the bulk structure.[18–24] Analysis of low-energy Ne ion scattering from a sample with about the same bulk composition as ours (3 at. %-Au-rich) yielded a Au concentration in the first two layers that is "essentially constant at 0.5 and 0, respectively" for temperature below 673 K.[18] (However, the data presented in Fig. 2 of Ref. 18 indicate that a 0.52 Au concentration in the first layer is consistent with the data and values given in the text indicate a 0.06 Au concentration in the second layer.) By 723 K, the Au concentration begins to *decrease* in the first layer and increase in the second. McRae and Malic,[2] using Auger spectroscopy, report that no changes in the Cu or Au signals are observed upon heating or cooling through the transition temperature. A room-temperature study combining scanning tunneling spectroscopy and low-energy neutral ion scattering concluded that the Au concentration in the surface layer is precisely 0.5, that the surface layer is never pure Cu even in small regions, that only double height steps occur with a height 0.15 Å larger than the bulk spacing, and that the surface is unreactive to oxygen and nitrogen.[19] Reichert *et al.*[20] analyzed the x-ray surface truncation rods of a 1.5 at. %-Cu-rich sample in the temperature range of $T_{bulk}+2$ K to $T_{bulk}+216$ K and concluded that the Au concentration of the top-most surface remains *constant* at about 0.44. This contrasts with a 3 at. %-Au-rich crystal where the Au composition *decreases* above T_{bulk}.[18]

Theoretical calculations of the surface composition of Cu_3Au (001) are in general agreement with experiments. The most recent study[22] finds that the Au-rich termination is favored by about 0.3 J/m^2 over a pure Cu termination, that the surface layer is buckled with the Au atoms relaxed outward from the bulk spacing and the Cu atoms inward, and a pairing of Cu atoms in the second layer. An abrupt decrease by several percent in the surface layer Au concentration at T_{bulk} and a further decrease at higher temperatures is predicted by the cluster-variation method.[23,24]

C. Kinetics of ordering

In bulk Cu_3Au, after rapidly quenching from the disordered state ($T>T_{bulk}$) to an annealing temperature $T<T_{bulk}$, long-range order develops in stages involving the formation and growth of antiphase domains. The average ordered domain size increases proportional to $t^{1/2}$ for stoichiometric and Au-rich samples[32–36] as expected from the Lifshitz-Allen-Cahn law[37,38] for curvature driven growth in a system with two degenerate phases. For times less than about 1000 s after the quench, the diffraction profile is best described by a Gaussian.[11,12] At later times the line shape is Lorentzian squared.[11,12,34] The earliest stage of ordering ($t<100$ s) (Ref. 39) is continuous and begins well above the classical spinodal temperature [$T_{bulk}-34$ K (Ref. 40)].

There have been comparatively few studies of the ordering kinetics at alloy surfaces as compared to the bulk. Ordering kinetics at the Cu_3Au (110) surface have been studied with LEED for the time regime from 10^2 to 10^5 s after a quench.[28] Ordering begins at about 6 K below the bulk transition temperature, domain size increases according to a t^n law, and occurs in three distinct time regimes, each characterized by a value of n. In each regime, n is considerably smaller than the bulk value of 1/2. In contrast, a domain-growth exponent $n=0.4\pm0.1$ was observed at the (111) surface of a 5000-Å-thick Cu_3Au film.[30] This value is essentially the same as the Lifshitz-Allen-Cahn theory value which is valid in the bulk.

III. EXPERIMENTAL METHODS

The copper-gold alloy sample was a cylinder of height 3.25 mm and diameter 10.1 mm. Three mounting slots were cut in the sides with a diamond saw. One end face was polished to a mirror finish with the final step being a 0.05 μm alumina slurry. The outward pointing surface normal was within 0.5° of the [001] direction and tilted midway between [0-10] and [1-10] directions in the surface. The sample consisted of six crystalline grains with in-plane orientations varying by up to 2.5° so that diffraction from individual crystallites was easily possible. The mosaic spread within each crystallite was about 0.25°. After cleaning in vacuum, the coherence length parallel to the surface of an individual grain was at least 500 nm. The bulk lattice constant at room temperature was determined by x-ray diffraction to be 0.3762 ± 0.0005 nm which corresponds to 28 ± 1 at. % Au.[41] The bulk order-disorder temperature was 644.5 ± 2 K, as discussed below, and corresponds to 29 ± 1.5 at. % Au.[1] Rutherford backscattering spectroscopy (RBS) yielded a composition of 27.9 ± 1.0 at. % Au.[42] RBS analysis was done at the same time on several other crystals.[30] One, the crystal used in a low-energy ion scattering study,[18] was found to be 29.0 ± 2.0 at. % Au, which is the same composition within experimental uncertainty as the crystal used by us.

The sample was mounted on a Ta plate with Ta tabs. Heating was by radiation from behind. Temperature was measured with a type-K thermocouple attached to one of the tabs. The thermocouple was calibrated in two ways. In the

first, the sample was transferred to an x-ray diffractometer with an oven that could be filled with nitrogen gas to insure an isothermal environment and avoid any temperature gradient between the sample surface and the thermocouple. The intensity of the (001) bulk x-ray reflection was used to monitor the order. In the second, carried out following the final x-ray measurements, an additional type-K thermocouple was placed directly in contact with the center of the crystal surface. Both methods yielded a bulk order-disorder temperature of 644.5 ± 2 K. At this temperature, type-K thermocouples have an accuracy of ± 2.8 K.[43]

Surface cleaning with 500 eV Ar^+ ions left the surface depleted of Au as reported previously.[2] The equilibrium surface composition was restored quickly by heating above 675 K for a few minutes but a sharp LEED pattern required heating for 20–30 min in general agreement with previous studies.[2–4,19,25–27] To eliminate the possibility of sulfur segregation,[4] which we found to occur in detectable amounts of about 925 K or higher, we kept the temperature below 800 K. The (001) surface of Cu_3Au is unreactive.[19] We found that, after cleaning in uhv, no detectable adsorption from the residual background occurred for several days. This is critical for the kinetic studies since they required more than 24 h.

X-ray-scattering experiments using 0.107 809 nm photons were carried out at Exxon beamline X10A at the National Synchrotron Light Source, Brookhaven National Laboratory.[44] Both x-ray scattering from the bulk and grazing incidence x-ray scattering (GIXS) for surface studies are possible. The outward surface normal is taken to be in the $[00l]$ direction and the $[h00]$ and $[0k0]$ directions are taken to be parallel to the surface. The critical angle for total external reflection from Cu_3Au is $\alpha_c = 0.33°$ and an incident angle $\alpha = 0.5°$ results in a penetration depth of about 30 nm. The beam size on the sample was set by slits to be about 5 mm by 0.5–2.0 mm; the precise size and shape varied with the scattering angle 2θ. The regions in reciprocal space that were studied in detail were the (100), (110), (101), (111), (001), and (002) reflections and the (00), (10), and (11) reciprocal-lattice rods [see Fig. 2(b)]. The x-ray data reported were acquired from individual grains in the mosaic but not all data is from the same grain. In all plots of the x-ray data, the reciprocal lattice is dimensioned using the room-temperature lattice constant and has not been corrected for thermal expansion. All data are normalized to the incident beam intensity which was monitored simultaneously.

The most sensitive measurements of the surface composition were made in a uhv chamber at the University of Maine using AES. A single-pass cylindrical mirror analyzer was used with a modulation amplitude of 1.0 V peak-to-peak and a 3 keV primary electron beam incident normally on the surface. Data where obtained for the energy range containing the Cu_{MVV} and Au_{NVV} transitions near 60 and 70 eV, respectively; we denote the peak-to-valley intensities of the peaks corresponding to these transitions by I_{Cu} and I_{Au}, respectively. The data were not corrected for a small temperature-dependent change in the shape of the background (probably caused by magnetic fields generated by the sample heater current) since this correction would change the ratio $R = I_{Cu}/I_{Au}$ by less than one-tenth of its statistical variation. The measured R as a function of temperature is shown in Fig. 3 and will be discussed later.

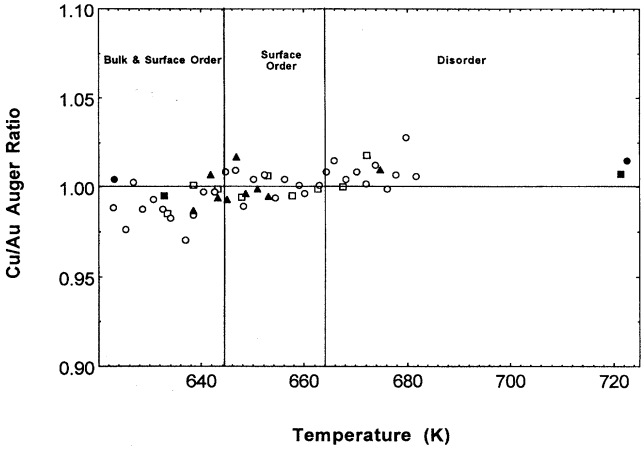

FIG. 3. Cu/Au Auger ratio as a function of temperature near the bulk and surface order-disorder transitions at T_{bulk} and T_{surf}, respectively.

A temperature controller was used to maintain the sample temperature to within ± 0.5 K of a preselected value during x-ray scattering and Auger spectroscopy measurements. Figure 4 shows a typical temperature history for one quench along with x-ray-diffraction data taken at the same time. The initial cooling rate is faster than 0.7 K/s. The maximum undershoot varied between about 1.5 K for the shallowest quenches to about 2.6 K for the deepest quench. In all cases, the temperature stabilizes to within 0.5 K of its final value T_f in less than 300 s.

Synchrotron x-ray scattering was also used for the kinetics experiments. Experiments were executed using the surface (100) superstructure reflection as a monitor of order near the surface. The (100) beam was examined by recording diffraction profiles in the h direction, keeping k and l fixed. The resolution in the h direction was set by the detector slits to be 0.003 or 0.000 75 $Å^{-1}$. Figure 4 shows data from the start of a typical measurement. Prior to the quench, the detector was set to scan only a small range in h centered on the

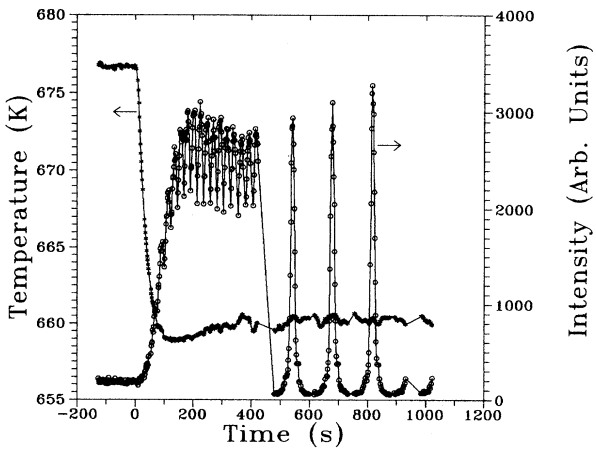

FIG. 4. Variation of the sample temperature and intensity of the (100) diffraction beam during the initial stages of a kinetics experiment. See the text for details.

position of the (100) peak; each short scan took about 20 s and did not usually include enough of the line shape to allow us to estimate the line width. This range was scanned continuously during the first few hundred seconds of the quench while T and (100) peak intensity were changing rapidly. In the case of Fig. 4, T decreases rapidly, undershoots T_f by about 1.4 K after about 120 s, and then rises to within 0.5 K of T_f after 300 s. The (100) intensity mirrors this behavior. There is an initial rapid rise to a maximum at the maximum T undershoot. The intensity then decreases slightly before starting to increase again. Following the initial rapid changes, at about 410 s in the case of Fig. 4, the diffractometer alignment was checked and the scan size was increased to include the entire (100) line shape. The first three scans across the entire peak are shown in Fig. 4. For all but two experiments, information about the (100) peak shape is only available from this time forward. Alignment was also checked periodically throughout the experiment.

IV. EXPERIMENTAL RESULTS

A. Surface composition

The composition across the entire sample surface was mapped using AES to insure that there were no differences in the compositions of the individual grains. The Cu concentration was constant to within $\pm 0.75\%$.

The average Cu composition is estimated to be 59% using the procedure described by Davis *et al.*[45] Although the accuracy of this estimate is probably not better than 5–10 %, it is good enough to show that the surface termination is much nearer 50% Cu than 100% Cu, if Λ is assumed to be in the range 5–10 Å (3–5 interlayer spacings).[26,46] However, an average composition of 59% is also consistent with the 56% Cu-44% Au surface termination extracted from x-ray data.[21]

More importantly, we have also made detailed measurements of the relative surface composition $R = I_{Cu}/I_{Au}$ as a function of temperature including measurements at 2 or 5 degree intervals between 623 and 683 K where the bulk and surface phase transitions occur. Data was obtained following a strict protocol because the approach to structural equilibrium is slow and because of the hysteresis associated with the first-order bulk transition. Thus, in each experiment, temperature was changed precisely at 1 h intervals and the Auger spectrum recorded just before the next temperature step. Our results indicate that the surface composition equilibrates much more rapidly than the crystallographic order as reported previously.[3,22] Figure 3 shows changes in the ratio $R = I_{Cu}/I_{Au}$ from its average value of $R_{av} = 1.13 \pm 0.01$ determined between 623 and 683 K; i.e., the vertical axis is R/R_{av}. The data lie slightly higher at higher temperatures. If we assume the change is linear, then R/R_{av} increases by 1.6% between 623 and 683 K. This corresponds to a small increase in the average Cu concentration of less than 0.005 (i.e., 0.5%). Whether this change occurs continuously cannot be decided from the data in Fig. 3. For example, the data are also consistent with nearly constant $R/R_{av} = 0.994$ for $T < 648$ K, an increase to $R/R_{av} = 1.000$ for 648 K $< T < 665$ K, and another small increase to $R/R_{av} = 1.009$ for 665 K $< T < 683$ K.

Above 683 K, we find that the surface concentration of Cu increases more strongly in agreement with earlier studies.[8,9,18] We note that the results of a recently reported analysis of x-ray-scattering data that concludes that the surface layer Au composition is independent of temperature[20,21] are not in agreement with our results or the results of Buck, Wheatley, and Marchut[18] using ion scattering data.

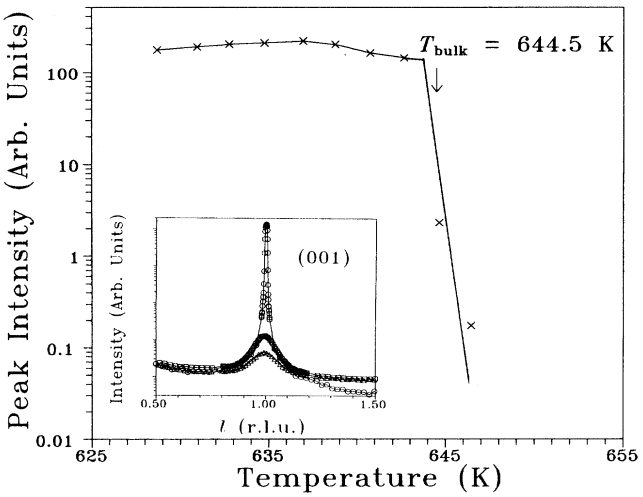

FIG. 5. Maximum intensity for the (001) beam as a function of temperature. T_{bulk} marks the temperature at which the intensity falls to 10% of its maximum value. The inset shows representative (001) line shapes above and below T_{bulk} (circles are at 633, squares at 650, and triangles at 656 K).

To summarize, although analysis of Auger data is not accurate enough to determine the absolute surface composition or its variation with depth, our results are consistent with a surface terminated by a 50% Cu and 50% Au layer, in agreement with most previous studies. Between 623 and 683 K, where two phase transitions occur (see below), there is an increase in the average Cu concentration of 0.005, at most. This change may take place incrementally, but higher precision measurements are needed to confirm this.

B. Quasiequilibrium bulk and surface transitions

The quasiequilibrium properties of the transition were studied by measuring line profiles of several reflections as the temperature was increased or decreased through the transition over a period of many hours. The degree of bulk long-range order was monitored by measuring the line profile of the out-of-plane (001) Bragg reflection. The in-plane (100) reflection was used to monitor surface long-range order. The inset in Fig. 5 shows several line profiles of the (001) bulk reflection at representative temperatures. These line profiles are Gaussian for $T < T_{bulk}$ and Lorentzian for $T > T_{bulk}$ as expected for the ordered and disordered phases, respectively. The (001) peak intensity of the Gaussian component versus temperature is shown in Fig. 5 which illustrates the rapid disappearance of the bulk compositional order at T_{bulk}. T_{bulk} is determined from temperature at which the intensity reaches 10% of its maximum value, which is 644.5 K. Other choices of the definition of T_{bulk}, such as the extrapolation of the intensity to zero or to 50% of the maximum, yield values within 2 K of 644.5 K.

Surface sensitive measurements were performed in the GIXS mode with the grazing angle of incidence $\alpha = 0.5°$.

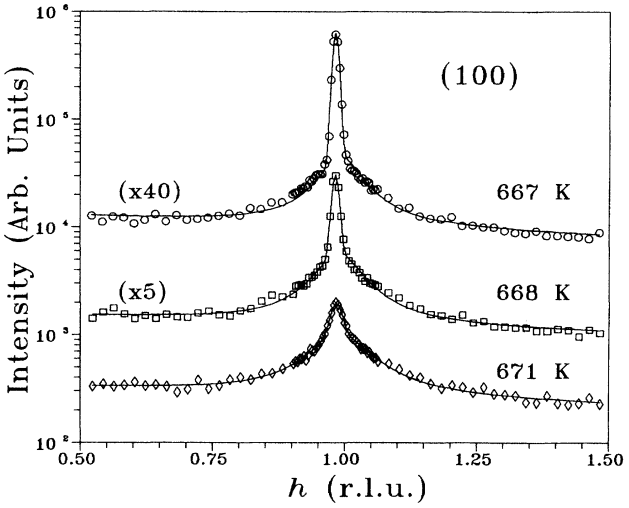

FIG. 6. Examples of (100) line shapes above T_{bulk}. Note the narrow, Gaussian component due to long-range order in the plane of the surface.

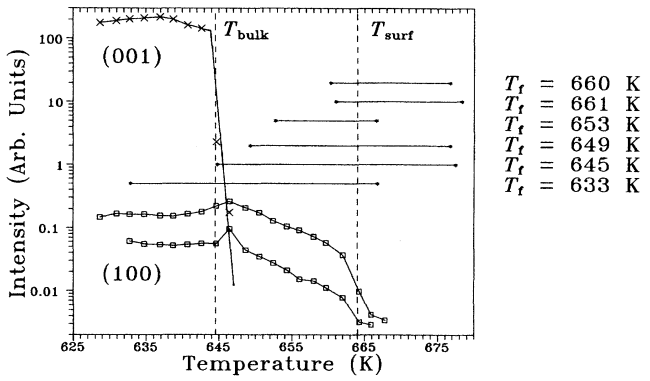

FIG. 7. Peak intensities from (001) bulk and (100) surface reflections. The surface reflection persists above the bulk transition temperature T_{bulk}. T_{surf} is defined as the temperature at which the (100) peak falls to 10% of its maximum value. The horizontal lines connect the initial and final temperatures of the quenches used for studies of the ordering kinetics; each line is labeled by the final temperature.

For this geometry, measurements across the (100) reflection in the h (or k) direction provide information about in-plane order (i.e., order parallel to the surface plane). Figure 6 shows typical line shapes of the (100) surface peak for various temperature above T_{bulk}. We refer to these measurements as *quasiequilibrium* since the sample was annealed at each temperature only until the change in intensity between two sequential scans was less than the signal to noise. Typically this required 1–2 h. As discussed in the next section, structural equilibrium is reached only after tens of hours. Note that the profiles in Fig. 6 consist of a sharp T-dependent Gaussian component and a broad T-independent Lorentzian component. The Lorentzian component is the contribution from the short-range order of the bulk disordered state. However, the Gaussian component is quite unexpected. It indicates the presence of long-range order in the sample despite the fact that the bulk is disordered in this temperature range. Since the intensity of the Gaussian component was found to be independent of the x-ray incident angle α, we attribute the long-range-order component to an ordered layer at the surface of the Cu_3Au sample.[8,31] Figure 7 presents peak intensities of the Gaussian component as a function of temperature for the (100) surface and (001) bulk reflections. The two sets of (100) data were obtained simultaneously from different crystallites in the mosaic structure. The most important feature of Fig. 7 is that long-range order disappears in the bulk at $T_{\text{bulk}}=644.5\pm2$ K but persists until $T_{\text{surf}}=664\pm2$ K in a layer near the surface.[8] We measure T_{surf} by the temperature at which the (001) intensity has reached 10% of its maximum value. The (100) intensity disappears altogether by 666 K and this temperature could be an alternative measure of T_{surf}. Thus x-ray-diffraction results indicate that order persists at temperatures above T_{bulk}. Surprisingly, we also observed similar behavior on a stoichiometric crystal later.[31]

The intensity along the (10) reciprocal-lattice rod which passes through the (100) surface and (101) bulk reflections [Fig. 2(b)] was also studied. Typical intensity data near (101) at $T=644$, 650, and 664 K are shown in Fig. 8(a). For $T<T_{\text{bulk}}$, the (101) beam consists of a single, sharp peak due to bulk long-range order. This intensity has the same T dependence shown for the (001) beam in Figs. 6 and 8. Above T_{bulk}, the profile becomes more complex. Along the (10) rod it broadens into a feature with two poorly resolved maxima that are symmetrically displaced from the (101) beam. Figure 8(b) shows a contour plot of this feature measured at 649 K in the hl plane containing the [100] and [001] directions. The diamond-shaped contours are due to the bulk short-range order caused by type-I antiphase domain boundaries[10,14] as shown schematically in Fig. 2(b). The more intense, cigar-shaped distribution concentrated along the (10) rod is the double-peaked feature in Fig. 8(a). The elongation in the [001] direction and the narrow width in the [100] and [010] directions are consistent with type-I antiphase domain boundaries that are oriented parallel to the (001) surface and have in-plane bulk long-range order. The temperatures for which the double-peaked feature is observed are plotted as stars in Fig. 1 and show that this feature occurs in the Cu_3Au II region of the phase diagram. Good fits to the intensities of the double-peaked features in Fig. 8(a) were obtained using two Gaussians of equal width plus a linear background. The splittings Δl between the Gaussians yield the mean spacings $M=a_0/\Delta l$ between domain boundaries oriented parallel to the surface; the M's so obtained range from $17a_0$ to $22a_0$ and are plotted as stars in Fig. 9. The standard deviation for each M, calculated from the Gaussian width, is comparable to, or slightly larger than, M; i.e., the order is poor. Figure 9 will be discussed in more detail later.

We now discuss evidence for an antiphase domain boundary structure observed on our sample for temperatures below T_{bulk}. Figures 10(a) and 10(b) show representative x-ray scans for the (001) bulk reflection at 621 K and the (021) beam at 633 K both taken along the l direction. Sharp satellites are observed in both cases—to second order for the (021) beam. It is evident that some type of long-range periodic structure develops perpendicular to the surface of our sample. The satellites disappear as the temperature is raised

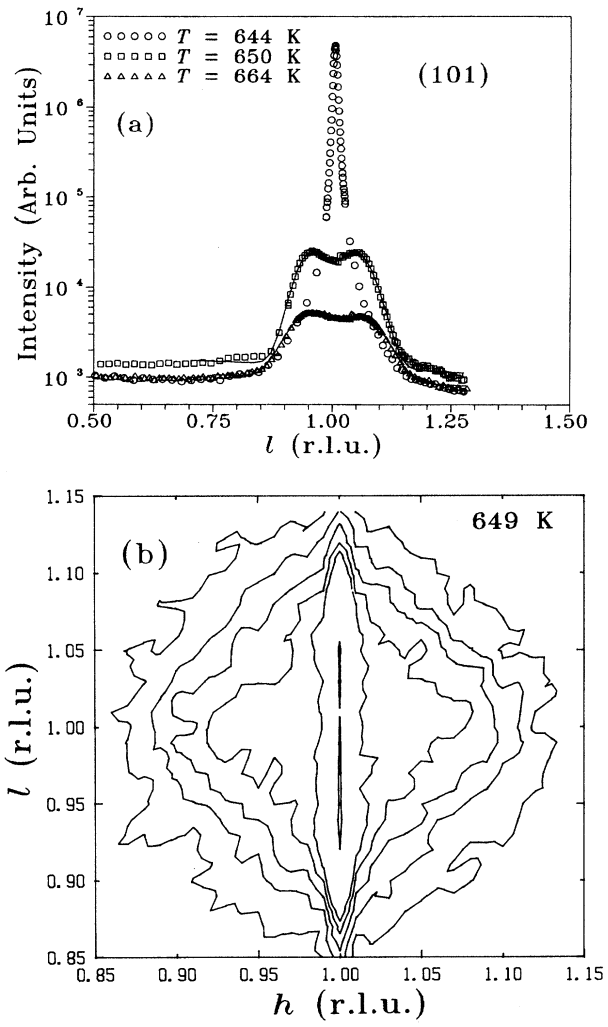

FIG. 8. (a) Typical scans through reciprocal space along the (01) reciprocal-lattice rod above and below the bulk transition temperature. The fits are discussed in the text. (b) Intensity contours in an lh plane passing through the (101) reflection; $T=649$ K.

above about 650 K or lowered below about 610 K. A detailed study of the temperature dependence and annealing behavior of these satellites was not carried out. The separations between the satellites and main peaks for the (001) and (021) reflections correspond to periods M of $11.4\,a_0$ and $10.5\,a_0$, respectively. These satellites are observed well inside the Cu_3Au I region of the phase diagram, rather than in the coexistence region (see Fig. 1). Since satellites in the l direction for these superstructure reflections cannot be caused by type-I antiphase domain boundaries [see Fig. 2(b)], they cannot be due to frozen-in bits of the Cu_3Au II phase; i.e., they cannot be explained with previous long-range periodic models that involve type-I antiphase domain boundaries.[13,16] We discuss possible origins of this long-range periodic structure, including their possible association with excess Au, below.

C. Kinetics of ordering

Thermal quenches were done from an initial temperature T_i in the solid solution (disordered) phase 3–14.5 K above

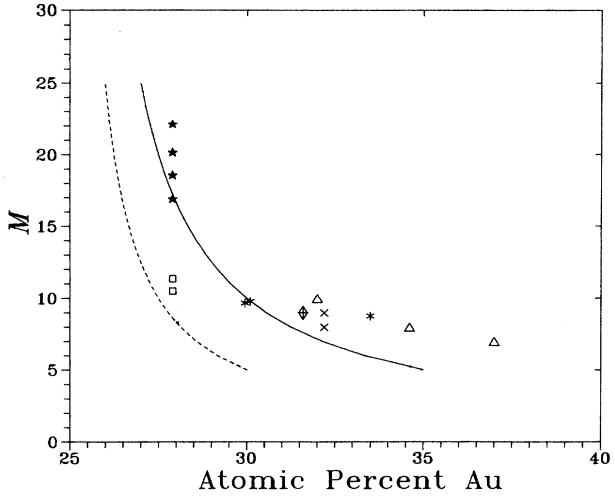

FIG. 9. Average spacings M of antiphase domain boundaries vs at. % Au (stars and squares from this work, +'s from Ref. 16, ×'s, Ref. 17).

T_{surf}, to an annealing temperature T_f as described in Sec. II. Data from the initial 1200 s of one experiment with $T_{bulk}<T_f<T_{surf}$ are shown in Fig. 4. In this case, the ordering is rapid enough for the x-ray intensity to follow the temperature undershoot; i.e., the intensity decreases slightly as the sample warms to its final temperature. For $T_f<T_{bulk}$, the response is more sluggish and a maximum does not occur during the undershoot; i.e., the initial ordering is slower.

Figure 11 shows typical (100) profiles after various elapsed times. Each profile consists of a narrow central peak centered on a broader background peak of very low intensity. This background peak is created during the initial stages of the quench and is not observed to change once full line profiles are measured beginning at about 250 s, even after 24 h. This suggests that some short-range disorder is frozen in during the initial part of the quench. The maximum and integrated intensities of the central peak increase up to the longest times studied. Simultaneously, the peak width decreases. Both observations are consistent with continued growth of an ordered domain. The background remains essentially constant but noisy because of the low count rate. Individual experiments were carried out for up to 10^5 s (27.8 h).

We find that a Gaussian yields the best fit to the long-range order portion of the (100) surface peak data shown in Fig. 11; i.e., the very low intensities of the short-range-order component and the background were ignored. The Lorentzian does not provide even a visibly good fit, although the Lorentzian squared is a reasonable fit at later times. At these times the Gaussian and Lorentzian-squared fits give the same results, within the 95% confidence limits of the full width at half maximum (FWHM) fit, for the average diameter of the ordered domains. For quenches to T_f with $T_{surf}>T_f>T_{bulk}$ where the maximum intensity is relatively small, the short-range-order component is still less than 5% of the maximum intensity I_m over most of the experiment. For experiments with annealing temperatures $T_f<T_B$ the short-range order intensity is less than 1% of I_m. In either of these cases the effect on the measured width is negligible. We removed the contribution of the resolution (transfer) function of the dif-

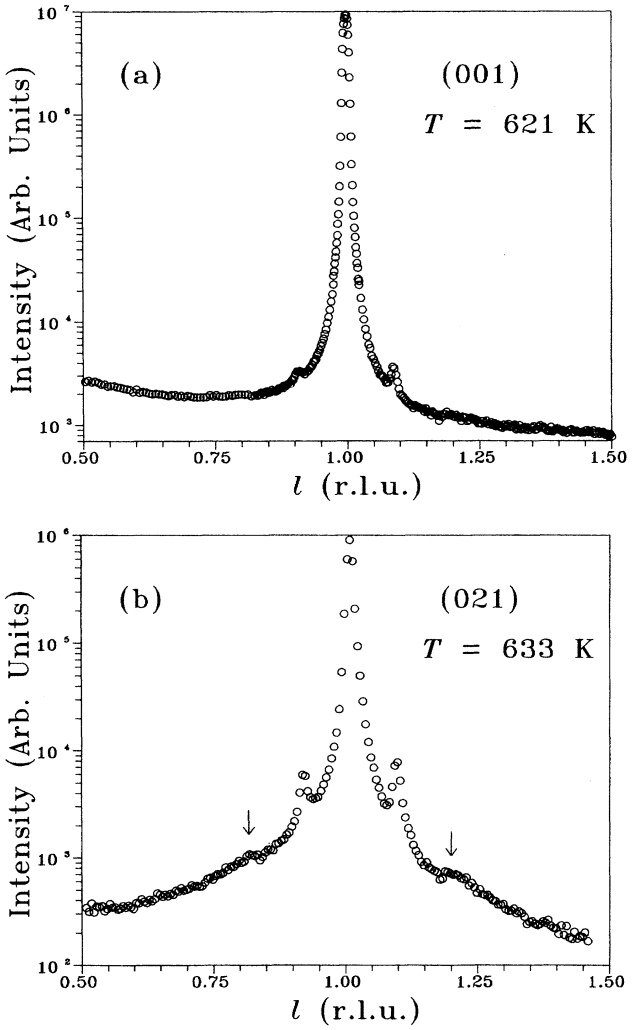

FIG. 10. Superstructure reflections with satellites while far below T_{bulk}. (a) (001) and (b) (021). These satellites cannot be explained by the Cu_3Au II phase.

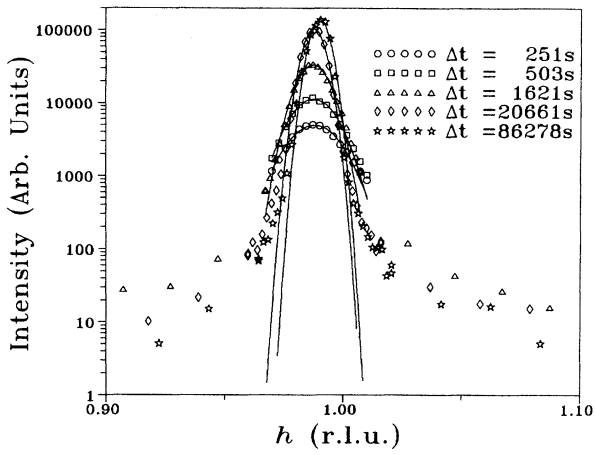

FIG. 11. Examples of (100) line shapes throughout a kinetics experiment. The short-range order does not change once formed, and bulk long-range order continues to grow in maximum intensity and integrated area and to narrow. The background is essentially constant.

fractometer to the measured width by assuming it to be a Gaussian. After the resolution function was removed, the resulting values for I_m, the FWHM, and integrated intensity were tabulated for each line shape along with the time for the data point closest to the peak.

The maximum intensity I_m is proportional to the square of the number of unit cells contributing to the line shape.[10] Figure 12(a) shows examples of the growth of I_m for two T_f, one at which only the surface layer is ordering and the other at which both the surface and bulk are ordering. Gaps in the data represent periods during which the synchrotron beam was not available. An initial rapid intensity rise, shown in Fig. 4, occurs primarily while the sample temperature is still decreasing. However, once the final annealing temperature is reached, the intensity increases more slowly as indicated by the data in Fig. 12(a). This behavior is typical of kinetics experiments in general.[19] We find no evidence for a time delay between the start of the quench and the start of ordering. This contrasts with experiments on the bulk kinetics of Cu_3Au where there is a time lag.[11,39] The maximum time lag consistent with our data is, at most, 20 s. This limit is set by the duration of the first scan after the start of the quench, and usually T is still greater than T_{surf} at this time.

I_m increases according to a power law with $n \leq 0.07$ for $t > 1000$ s when T_f is in the range where only the surface layer orders. For $T_f < T_{bulk}$, I_m also increases slowly but cannot be described by a power law except perhaps for the very longest times studied, $t > 5 \times 10^4$ s.

The FWHM determined for (100) peak data like those in Fig. 11 provide information about the growth of the harmonic mean of the domain sizes W as measured along the h direction. Figure 12(b) show examples for quenches with $T_{bulk} < T_f < T_{surf}$ and with $T_f < T_{bulk}$. W increases most slowly for quenches into the ordered surface phase, more rapidly for quenches near T_{bulk}, and appears to be slow again for quenches deeper below T_{bulk}. A possible explanation for this is that, not only do a larger number of nuclei form for the deeper quenches, but diffusion is slower. Quenches to temperatures in the range $T_{surf} > T_f > T_{bulk}$ where only the surface orders, show very slow growth that can be described by a power law with exponent $n \leq 0.07$ for $t > 2000$ s. For quenches below T_{bulk}, the initial growth of W is described by a power law with $n = 0.20 \pm 0.05$ but the growth slows substantially at longer times. Lines with $t^{1/2}$ and $t^{1/3}$ are shown in Fig. 12(b) for comparison. In all cases the growth rate is much slower than the $n = 1/2$ value predicted by Lifshitz,[37] and Allen and Cahn[38] for an ordering process involving two energetically equivalent antiphase domains, and observed for bulk Cu_3Au.[32–36] The growth exponent of 1/3 is expected if the growth is limited by diffusion.[47]

We note that W and I_m have different growth rates with that of I_m being higher. This indicates that the rates of growth parallel and perpendicular to the surface are different. Further insight can be gained by comparing W and the integrated intensity ΣI. For the (100) data in Fig. 11, the detector aperture was large enough to integrate over both the k and l directions so that ΣI is proportional to $N_h N_k N_l$ where $N_{h'}$, $N_{k'}$, and N_l are the average number of lattice spacing

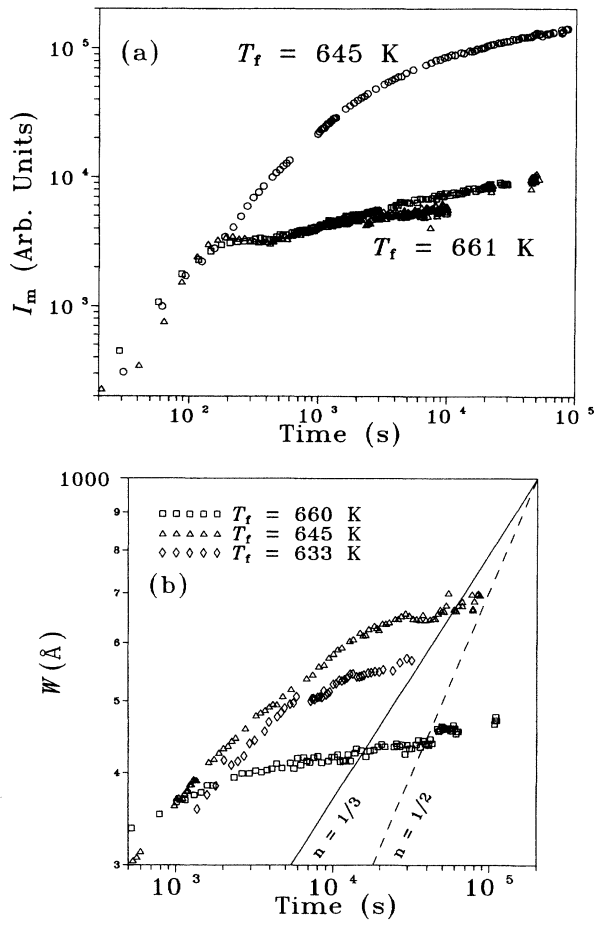

FIG. 12. Summary of kinetics experiments. (a) Growth of the (100) peak intensity I_m. (b) Growth of average domain widths W in the h direction versus time for quenches from the disordered state.

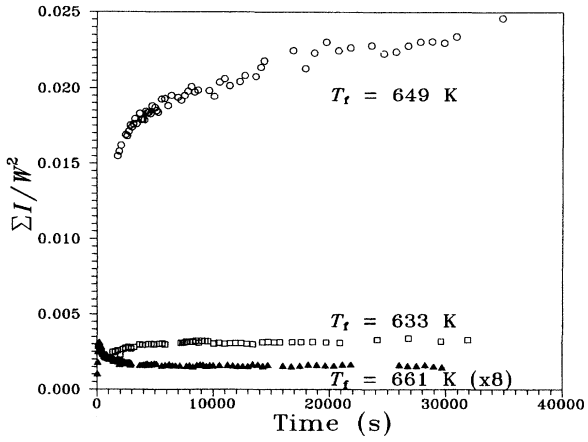

FIG. 13. $\Sigma I/W^2$ vs time. $\Sigma I/W^2$ is proportional to the average size of ordered domains measured perpendicular to the surface.

in the h, k, and l directions, respectively. W is proportional to N_h only. Because of the symmetry of the surface, we also expect $N_h = N_k$. Thus, assuming that the structure factor does not change significantly, a plot of $\Sigma I/W^2$ vs time will provide a measure of the growth rate of $N_{l'}$, i.e., the mean size of ordered regions perpendicular to the surface plane. Representative results are shown in Fig. 13. For a very shallow quench to $T_f = 661$ K (black triangles), $\Sigma I/W^2$ remains constant except for a maximum that occurs during the temperature undershoot that occurs during the quench (see the discussion associated with Fig. 4). For this case, once the final temperature is reached, the thickness of the ordered surface layer remains nearly constant while the long-range order increases parallel to the surface plane. However, for all deeper quenches studied, $\Sigma I/W^2$ increases even for the longest times. Examples are shown in Fig. 13 for quenches to 649 K (circles) and 633 K (squares). [Unfortunately, quantitative comparison of absolute intensities is not possible because the kinetics data were taken during several running periods at the synchrotron. Under these circumstances, the mosaic structure sampled in each set of experiments varies slightly. The (100) intensity data shown in Fig. 7 illustrate the typical range of variations due to the mosaic structure.]

Finally, we note that our measurements were carried out on a single sample and kinetics studies are often sensitive to properties that might be specific to each sample. In our case these might include a slight misorientation of the surface, the mosaic structure, or undetectable amounts of contamination by sulfur or some other impurity. We cannot rule out such effects completely, but several factors suggest that they may not be significant. First, the kinetics remained unchanged over a period of about two years during which the sample was removed from the uhv chamber, remounted several times, sputter cleaned frequently, heated above the transition temperature in vacuum many hundreds of times and in a nitrogen atmosphere several times. Also, the same kinetic and thermodynamic behavior was observed for different grains of the mosaic structure. Finally, studies of our crystal by another group[21] are generally consistent with our results where comparison is possible.

V. DISCUSSION

A. Surface segregation and ordering

The surface phase transition for our Au-rich alloy occurs at a temperature of 664–666 K that is essentially the same as the transition temperature for stoichiometric bulk Cu_3Au (663 K). This suggests the following simple model: a surface layer of stoichiometric Cu_3Au forms at the (001) surface and has an order-disorder transition near that of bulk Cu_3Au. This results in an ordered layer at the surface in the temperature interval 644.5 K$<T<$665 K; i.e,. between the bulk ordering temperatures of $Cu_{72}Au_{28}$ and Cu_3Au.

The composition of the surface layer of ordered $Cu_3Au(100)$ is known to be of the 50% Cu-50% Au type. This has been established through numerous experimental[18–21] and theoretical[22–24] studies. In fact, it has been shown that Au segregates to the surface of most Cu-Au alloys.[26,48,49] Our Auger spectroscopy results discussed above show that there is less than a 0.5% increase in the near-surface Cu concentration as the temperature is raised through the bulk and surface transition temperatures. This, coupled with the results of Buck, Wheatley, and Marchut,[18] who used a crystal with the same bulk composition as ours,

and the theoretical result that the 50% Cu-50% Au is energetically favored by about 0.3 J/m^2,[22] suggest that the (001) surface composition of Au-rich Cu_3Au crystals is very near that of stoichiometric Cu_3Au. Additional support for this model is provided by Kumar and Bennemann[23] who argue that the results of Buck, Wheatley, and Marchut[18] are evidence of stronger long-range order at the surface than in the bulk. A larger increase in the surface Cu concentration begins only at much higher temperatures, 725–775 K.

Thus, when the sample is at the temperature from which the quenches began, the surface was already at a composition close to that in the ordered state (50% Cu-50% Au) rather than at the average bulk composition (72% Cu). As the temperature is lowered, a layer with composition near that of Cu_3Au nucleates and grows into the bulk. As discussed below, this layer is actually Cu_3Au II because of the presence of type-I antiphase domain boundaries. Once the temperature reaches the bulk transition temperature of $Cu_{72}Au_{28}$, ordering begins in the bulk.

B. Long-period structures at the (001) surface

We obtain information about long-range periodic structures at the (001) surface including the observation of another phase.

There is a very strong preference for type-I boundaries that are oriented parallel to the surface as shown most clearly in the cigar-shaped intensity feature in Fig. 8(b). In the bulk, where all orientations are equally probable, the diffraction has characteristic diamond-shaped intensity distributions about the locations of the superstructure beams as shown in Fig. 2(b). Since they are created by half-diagonal glides along $\langle 110 \rangle$ directions, the intersection of a type-I boundary with the (001) surface would result in the formation of a single height step. However, scanning tunneling microscopy[19] clearly shows that only double height steps form on this surface. We conclude that type-I boundaries that intersect the surface are unstable. The double-peaked intensity in Fig. 8(a) also indicates that there is a weak interaction between type-I boundaries that results in partial ordering. The mean spacings M that we determined, Figs. 1 and 9, fit in with the general dependence on Au concentration established by previous studies of the Cu_3Au II phase.[16,17] The solid line in Fig. 11 is the prediction of a model due to van der Perre *et al.*[50] in which the excess Au atoms are incorporated into the type-I antiphase domain boundary.

The existence of a long-range periodic structure observed in the Cu_3Au I phase region (see Fig. 1) is demonstrated by the sharp satellites shown in Fig. 10. We note first that, since these sharp satellites are in the l direction around (001) and (021) superstructure reflections, they cannot be due to type-I antiphase domain boundaries or regions of Cu_3Au II phase[13,16] [see Fig. 2(b)]. From Fig. 9, the values of M calculated from these data lie well below the van der Perre curve. Instead, they fall very close to the dashed line which is calculated assuming that all of the excess Au is incorporated into an extra 50% Cu-50% Au layer located at the domain boundary. But this is just a type-II domain boundary.

This observation has important implications for the ordering mechanism in our sample. We propose an extension to this line of thinking which still suggests bulk long-range-order structure, but from type-II rather than type-I antiphase domain boundaries. The model for this is as follows: (1) Ordering begins at the surface at a temperature of 666 K. It is reasonable to assume that this ordering layer is stoichiometric Cu_3Au because the transition temperature is quite close to that of bulk stoichiometric Cu_3Au, $T_0 = 663$ K. (2) As the temperature is lowered toward the bulk transition temperature, $T_{\text{bulk}} = 644.5$ K, the ordered layer grows deeper into the sample. (3) Due to the finite solubility of Au in Cu_3Au, some of the Au is randomly distributed through the growing ordered domain, but most of it is carried into the bulk at the order-disorder interface. (4) When the Au concentration reaches a high enough level an extra 50% Cu-50% Au layer forms, creating a type-II boundary. (5) As the growth continues into the bulk, steps (3) and (4) are repeated forming a periodic structure.

Once formed, type-II domain boundaries will be harder to anneal out since this requires a larger energy cost than type-I boundaries plus a substantial mass transport. Thus, sharp satellites result for the (001) and (021) beams at temperatures 15 K into the Cu_3Au I region of the phase diagram. Those at (101) are not sharp because they are aligned with the splitting due to the type-I antiphase domain boundaries, i.e., Cu_3Au II phase. The (021) satellites decrease in intensity and the central peak increases if the temperature is lowered from 633 to 623 K.

This sharp satellite profile suggests large antiphase domains with a fairly regular size distribution. This regularity can be due to the process outlined above in steps (3) and (4). One physical effect causing this could be the strain field from the atomic size mismatch between Cu and Au. The formation of antiphase domain boundaries, though costing configurational energy due to an increase in high-energy Au-Au bonds, will relieve strain. These boundaries thus become energetically favorable once a large enough strain field has been established from the excess Au atoms in the matrix.

C. Ordering kinetics at Cu_3Au surface

Growth of an ordered surface film occurs in two stages following a quench from the disordered state to a T_f at which only the surface can order. The first stage is rapid formation of a partially ordered film during the first few hundred seconds of the transient cool down period. This is followed by a second, temperature-dependent, stage of slow growth. For temperatures very near T_f, the thickness of the surface layer does not change significantly but there is a slow increase in lateral order according to a power law with an exponent of about 0.04. For quenches deeper than 655 K, the ordering also continues to improve deeper into the bulk. Data between 655 and 660 K needed to study the transition between these growth regimes are not available. The film contains antiphase domain boundaries with type-I character that are oriented parallel to the surface with a tendency to develop weak long-range order with periodicity of about 20 bulk lattice constants. However, type-I boundaries are not involved in the lateral ordering process.

At lower temperatures, where the bulk can order simultaneously with the surface film, the growth remains slow but is

no longer described by a power law and the thickness of the ordered region increases throughout the annealing period. Sharp satellites on the (001) and (021) beams provide strong evidence for the development of a highly ordered array of type-I antiphase domain boundaries oriented parallel to the surface.

It is tempting to explain the slow growth as due to the excess Au atoms behaving like impurities. For example, similar behavior is obtained for the Ising model with nonconserved order parameter where the addition of static, random impurities[51,52] pins the domain walls, selects a maximum average domain width, and severely slows down the growth. However, in our case, extrapolation of the diffusivity data of Benci, Germagnoli, and Schianchi[53] to the temperature range of our experiments suggests that the Au atoms are unlikely to be fixed but will diffuse with root-mean-square displacements of about one lattice constant in 10 s. However, mobile impurities are also known to impede growth. Mouritsen and Shah[54] have shown that, for a pure system which follows the Lifshitz-Allen-Cahn growth law, a mobile impurity concentration of only 0.5% is sufficient to slow the kinetics consistent with $n=\ln t$. Their ln-ln plot of average domain size versus time (Fig. 4 in Ref. 54) is consistent with an $n=1/8$ growth law, which Lipowsky and Huse[55] have shown also describes diffusion-limited growth of wetting layers in binary fluid mixtures.

Unfortunately, studies of the effects of both excess Cu and Au on the ordering kinetics of bulk Cu_3Au show that a Au impurity concentration alone cannot explain the slow growth rate in our sample. Shannon, Harkless, and Nagler[56] find that extra Cu in thin films of Cu_3Au does slow the kinetics to $n=0.2$ growth. In contrast, however, Rase and Mikkola[36] have shown that excess Au has no effect on the $n=0.5$ coarsening law. They studied three Au compositions, one essentially the same as ours. The only effect of excess Au was to limit the size of the domains to about 133 a_0 for a 27.9% Au sample and about 36 a_0 for a 31.5% Au sample.

In terms of the model we described above, we expect the boundary between the ordering surface film and the underlying bulk to be a type-II antiphase boundary. At the start of ordering, the surface composition is very nearly 50% Cu and 50% Au and acts as a template for development of the order. The film grows rapidly into the crystal as nearly stoichiometric Cu_3Au with excess Au accumulating at the interface. When this accumulation is large enough, an extra 50% Cu-50% Au layer forms and becomes the template for growth of an additional layer. In the bulk, the type-II domain boundaries are separated by about 10–11 a_0 for our crystal. Near the surface this spacing will be larger because the near-surface Au composition may be less than its bulk value 28% and because the initial growth may be too rapid for all the excess Au to reach the interface. Once one (or more) type-II boundaries have formed it will be quite stable because of the large amount of mass transport required to remove it. These boundaries may also act as diffusion barriers for additional redistribution of Au atoms trapped in the intervening regions.

Our model has some features in common with the two phase mixture model proposed by Williams[57] to explain ordering in Au-rich bulk Cu_3Au alloys. In his model, the ordered state is described as a mixture of pure Cu_3Au I and a solid solution containing the excess Au in type-II boundaries. As the sample is heated, the type-II boundaries become the nuclei for generation of a solid solution with type-I boundaries. It is interesting to note that this model shares characteristics of both first- and higher-order transitions since two distinct phases coexist as for a first-order transition, but there are long-wavelength fluctuations characteristic of a continuous transformation. Additional measurements on the ordering are needed to clarify the situation further.

VI. SUMMARY AND CONCLUSIONS

We have described an experimental study of the order-disorder transitions at the (001) surface of a Au-rich Cu_3Au crystal including data about the kinetics of the transitions. The actual composition of the crystal studied is $Cu_{72}Au_{28}$. Structural ordering in this material requires many hours. Thus care must be taken to minimize hysteresis effects associated with the recent thermal history. The quasiequilibrium properties were studied with x-ray scattering and Auger spectroscopy.

The first-order bulk order-disorder transition occurs at $T_{\text{bulk}}=644.5\pm2$ K in good agreement with previous studies. This is about 18–19 K lower than for stoichiometric Cu_3Au. A phase, possibly metastable, with a translational periodicity of about 10 unit cells is observed to at least 15 K below T_{bulk}. A model involving type-II antiphase domain boundaries is discussed.

A layer near the surface remains ordered until $T_{\text{surf}}=664\pm2$ K; i.e., about 20 K above T_{bulk}. This observation is different than reported for previous studies of stoichiometric $Cu_3Au(001)$ where the surface layer is generally reported to disorder continuously at temperatures below T_{bulk}. In the temperature range $T_{\text{bulk}}<T<T_{\text{surf}}$ where only the surface layer is ordered, the crystal structure appears to be similar to Cu_3Au II; i.e., ordered arrays of type-I antiphase domain boundaries are formed. The value of T_{surf} and previous work[18] on a crystal of the same bulk composition suggest that the surface layer could be Cu_3Au, but our composition measurements are not able to confirm this. However, we do find that the average composition in the near-surface region of $Cu_{72}Au_{28}(001)$ changes by less than 0.5% during the surface and bulk phase transitions. High-temperature scanning tunneling microscope measurements could provide valuable insights into the structure at the surface since it appears that the Au and Cu atoms can be distinguished.[19]

The growth of ordered domains following quenches from the disordered state above T_{surf} is very slow compared to all previous studies on Cu-Au alloys. The diffracted intensities continue to increase even for the longest times studied ($\approx$24 h). Domain growth following quenches to temperatures $T_{\text{bulk}}<T_f<T_{\text{surf}}$, where only the surface layer is ordered, is described by a power law t^n with $n=0.04$ for $t>300$ s. The ordering occurs primarily parallel to the surface. Domain growth for quenches to below T_{bulk} does not follow a power law and slows substantially at the longest times studied. The incorporation of excess Au in low mobility type-I antiphase domain boundaries is one possible reason for the slow growth. A short-range-order component of the diffracted intensities forms during the first few hundred

seconds of a quench and does not change significantly even for the longest times studied.

ACKNOWLEDGMENTS

The aid of K. L. D'Amico and C. H. Lee with data acquisition is gratefully acknowledged. We thank W. E. Wallace for doing the RBS analysis. One of the authors (S.B.R.) would like to acknowledge many helpful discussions with S. R. McKay. Financial support for this research was provided in part through National Science Foundation Grant No. DMR-8803529. S. B. Rivers also received financial support from the University of Maine and Exxon. H. H. Hung received financial support from the Synchrotron Radiation Research Center, Taiwan. This research was carried out in part at the National Synchrotron Light Source, Brookhaven National Laboratory, which is supported by the U.S. Department of Energy, Division of Materials Sciences and Division of Chemical Sciences.

---

*Present address: Department of Ceramics, Rutgers University, Piscataway, NJ 08855.

†Permanent address: Synchrotron Radiation Research Center, Hsinchu, Taiwan.

[1] H. Okamoto, D. J. Chakrabarti, D. E. Laughlin, and T. B. Massalski, Bull. Alloy Phase Diagrams **8**, 454 (1987).

[2] E. G. McRae and R. A. Malic, Surf. Sci. **148**, 551 (1984).

[3] K. D. Jamison, D. M. Lind, F. B. Dunning, and G. K. Walters, Surf. Sci. Lett. **159**, L451 (1985).

[4] S. F. Alvarado, M. Campagna, A. Fattah, and W. Uelhoff, Z. Phys. B **66**, 103 (1987).

[5] H. L. Dosch, L. Mailander, A. Lied, J. Peisl, F. Grey, and R. E. Weber, Phys. Rev. Lett. **23**, 2382 (1988); H. L. Dosch, L. Mailander, H. Reichert, J. Peisl, and R. I. Johnson, Phys. Rev. B **43**, 13 172 (1991).

[6] R. Lipowsky, J. Appl. Phys. **55**, 2485 (1984).

[7] R. Lipowsky and W. Speth, Phys. Rev. B **28**, 3983 (1983).

[8] S. B. Rivers, W. N. Unertl, H. H. Hung, and K. S. Liang, in *Kinetics of Phase Transformations*, edited by M. O. Thompson, M. Aziz, and G. B. Stephenson, MRS Proceedings No. 205 (Materials Research Society, Pittsburgh, 1992), p. 145.

[9] S. B. Rivers, Ph.D. thesis, University of Maine, 1993.

[10] B. W. Warren, *X-Ray Diffraction* (Dover, New York, 1990), Chap. 12.

[11] S. E. Nagler, R. E. Shannon, Jr., C. R. Harkless, M. A. Singh, and R. M. Nicklow, Phys. Rev. Lett. **61**, 718 (1988).

[12] R. E. Shannon, Jr., S. E. Nagler, C. R. Harkless, and R. M. Nicklow, Phys. Rev. B **46**, 40 (1992).

[13] M. J. Marcinkowski and L. Zwell, Acta Metall. **11**, 373 (1963).

[14] J. M. Cowley, *Diffraction Physics*, 2nd revised ed. (North-Holland, Amsterdam, 1990); Phys. Rev. **77**, 669 (1950); J. Appl. Phys. **21**, 24 (1950).

[15] F. N. Rhines, W. E. Bond, and R. A. Rummel, Trans. Am. Soc. Met. **47**, 578 (1955).

[16] R. E. Scott, J. Appl. Phys. **35**, 2112 (1960).

[17] H. L. Yakel, J. Appl. Phys. **33**, 2439 (1962).

[18] T. M. Buck, G. H. Wheatley, and L. Marchut, Phys. Rev. Lett. **51**, 43 (1983).

[19] H. Niehus and C. Achete, Surf. Sci. **289**, 19 (1993).

[20] H. Reichert, P. J. Eng, and I. K. Robinson, Phys. Rev. Lett. **74**, 2006 (1995).

[21] I. K. Robinson and P. J. Eng, Phys. Rev. B **52**, 9917 (1995).

[22] W. E. Wallace and G. J. Ackland, Surf. Sci. Lett. **275**, L685 (1992).

[23] V. Kumar and K. H. Bennemann, Phys. Rev. Lett. **53**, 278 (1984).

[24] J. M. Sanchez and J. L. Moran-Lopez, Surf. Sci. Lett. **157**, 297 (1985); J. M. Sanchez and J. L. Moran-Lopez, Phys. Rev. B **32**, 3534 (1985).

[25] V. S. Sundaram, R. S. Alben, and W. D. Robertson, Surf. Sci. **46**, 653 (1974); V. S. Sundaram, B. Farrell, R. S. Alben, and W. D. Robertson, Phys. Rev. Lett. **31**, 1136 (1973).

[26] H. C. Potter and J. M. Blakely, J. Vac. Sci. Technol. **12**, 635 (1975).

[27] B. Gans, P. A. Knipp, D. D. Koleske, and S. J. Seibner, Surf. Sci. **264**, 81 (1992).

[28] E. G. McRae, T. M. Buck, R. A. Malic, and W. E. Wallace, Surf. Sci. Lett. **238**, L481 (1990).

[29] Y. Huang and J. M. Cowley, Surf. Sci. **285**, 42 (1993); **289**, 340 (1993).

[30] X.-M. Zhu, R. Feidenhans'l, H. Zabel, J. Als-Nielsen, R. Du, C. P. Flynn, and F. Grey, Phys. Rev. B **37**, 7157 (1988); X. M. Zhu, I. K. Robinson, E. Vlieg, H. Zabel, J. A. Dura, and C. P. Flynn, J. Phys. (Paris) Colloq. **50**, C7-283 (1989).

[31] K. S. Liang, H. H. Hung, S. L. Chang, Z. Fu, S. C. Moss, and K. Oshima, in *Surface X-Ray and Neutron Scattering*, edited by H. Zabel and I. K. Robinson (Springer-Verlag, New York, 1992), p. 65.

[32] G. E. Poquette and D. E. Mikkola, Trans. TMS-AIME **245**, 743 (1969).

[33] T. Hashimoto, K. Nishimura, and Y. Takeuchi, J. Phys. Soc. Jpn. **45**, 1127 (1978).

[34] Y. Noda, S. Nishihara, and Y. Yamada, J. Phys. Soc. Jpn. **53**, 4241 (1984).

[35] M. Sakai and D. E. Mikkola, Metall. Trans. **2**, 1635 (1971).

[36] C. L. Rase and D. E. Mikkola, Metall. Trans. A **6**, 2267 (1974).

[37] I. M. Lifshitz, Sov. Phys. JETP **15**, 939 (1962).

[38] S. M. Allen and J. W. Cahn, Acta Metall. **27**, 1085 (1979).

[39] K. F. Ludwig, G. B. Stephenson, J. L. Jordan-Sweet, J. Mainville, Y. S. Yang, and M. Sutton, Phys. Rev. Lett. **61**, 1859 (1988).

[40] H. Chen, J. B. Cohen, and R. Ghosh, J. Phys. Chem. Solids **38**, 855 (1977).

[41] W. B. Pearson, *Handbook of Lattice Spacings and Structures of Metals and Alloys* (Pergamon, Oxford, 1958).

[42] W. Wallace (unpublished).

[43] Natl. Inst. Stand. Technol. Mono. **175**, 153 (1993).

[44] K. L. D'Amico and K. S. Liang (unpublished).

[45] L. E. Davis, N. C. MacDonald, P. W. Palmberg, G. E. Riach, and R. E. Weber, *Handbook of Auger Electron Spectroscopy*, 2nd. ed. (Physical Electronics Industries, Eden Prairie, 1976).

[46] M. P. Seah and W. A. Dench, Surf. Interface Anal. **1**, 2 (1979).

[47] I. M. Lifshitz and V. V. Slyozov, J. Phys. Chem. Solids **19**, 35 (1961).

[48] J. M. McDavid and S. C. Fain, Surf. Sci. **52**, 161 (1975).

[49] R. A. Van Santen, L. H. Toneman, and R. Bouman, Surf. Sci. **47**, 64 (1975).

[50] G. van der Perre, H. Goeminne, R. Geerts, and J. van der Planken, Acta Metall. **22**, 227 (1974).

[51] D. A. Huse and C. L. Henley, Phys. Rev. Lett. **54**, 2708 (1985).

[52] G. S. Grest and D. J. Srolowitz, Phys. Rev. B **32**, 3014 (1985).
[53] S. Benci, G. Germagnoli, and G. Schianchi, J. Chem. Phys. Solids **26**, 687 (1965).
[54] O. G. Mouritsen and P. J. Shah, in *Kinetics of Ordering and Growth at Surfaces*, edited by M. G. Lagally (Plenun, New York, 1990), p. 45.
[55] R. Lipowsky and D. A. Huse, Phys. Rev. Lett. **57**, 353 (1986).
[56] R. F. Shannon, C. R. Harkless, and S. E. Nagler, Phys. Rev. B **38**, 9327 (1988).
[57] R. O. Williams, Metall. Trans. A **11**, 247 (1980).